THE JOURNAL OF PHYSICAL CHEMISTRY B

Article

pubs.acs.org/JPCB

From Solution to the Gas Phase: Factors That Influence Kinetic Trapping of Substance P in the Gas Phase

Kyle L. Fort,[†] Joshua A. Silveira,[†] Nicholas A. Pierson,[‡] Kelly A. Servage,[†] David E. Clemmer,[‡] and David H. Russell*[,†]

[†]Department of Chemistry, Texas A&M University, College Station, Texas 77843, United States

[‡]Department of Chemistry, Indiana University, 800 East Kirkwood Avenue, Bloomington, Indiana 47405, United States

Supporting Information

ABSTRACT: Substance P (RPKPQQFFGLM-NH_2) $[M + 3H]^{3+}$ ions have been shown to exist as two conformers: one that is kinetically trapped and one that is thermodynamically more stable and therefore energetically preferred. Molecular dynamics (MD) simulations suggested that the kinetically trapped population is stabilized by interactions between the charge sites and the polar side chains of glutamine (Q) located at positions 5 and 6 and phenylalanine (F) located at positions 7 and 8. Here, the individual contributions of these specific intramolecular interactions are systematically probed through site-directed alanine mutations of the native amino acid sequence. Ion mobility spectrometry data for the mutant peptide ions confirm that interactions between the charge sites and glutamine/phenylalanine (Q/F) side chains afford stabilization of the kinetically trapped ion population. In addition, experimental data for proline-to-alanine mutations at positions 2 and 4 clearly show that interactions involving the charge sites and the Q/F side chains are altered by the cis/trans orientations of the proline residues and that mutation of glycine to proline at position 9 supports results from MD simulations suggesting that the C-terminus also provides stabilization of the kinetically trapped conformation.

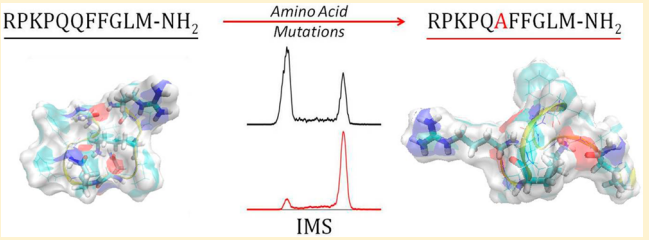

INTRODUCTION

Peptide and protein structures are dictated by intrinsic intramolecular interactions involving hydrophobic and hydrophilic regions in their molecules, interactions with other species in the solution (e.g., cations, anions, detergents, and other solubilizing agents), and interactions with the solvent. Unraveling the contributions of each individual interaction and determining how their collective effects alter conformational preferences are major challenges to understanding peptide/protein structure/function relationships. Studies of gas-phase, solvent-free biomolecule ions provide a means to investigate conformational preferences because intra- and intermolecular interactions are effectively decoupled under these conditions.[1−4] Ion mobility-mass spectrometry (IM-MS) is increasingly being used for studies of gas-phase peptide/protein ion conformations and provides unparalleled capabilities for deconvoluting conformational heterogeneity in these systems. One potential concern with this approach is that in transitioning from solution to the gas phase via the electrospray ionization (ESI) process biomolecules must undergo dehydration reactions that may affect conformer preferences and population distribution.[1,5,6] For example, as solvent is removed, the stabilization afforded by water is diminished, and intramolecular electrostatic interactions (e.g., salt bridges and/or hydrogen bonds) become increasingly more important.[7,8] On the other hand, there is a growing body of evidence that suggests "nativelike" states of gaseous ions are kinetically trapped in local minima on the potential energy surface because of evaporative cooling and reduced rates of interconversion among energetically accessible states.[7−21] Of critical importance to the study of conformational preferences of biomolecules by IM-MS is the preservation of these "nativelike", or kinetically trapped, conformations. Skinner et al.[22] and Breuker[7] interpreted results from electron capture dissociation (ECD) studies as evidence that intramolecular interactions between charge sites and polarizable amino acid side chains are formed upon complete desolvation and that these interactions afford stability to kinetically trapped conformations. Breuker recently reported ECD data for horse and tuna cytochrome c that show differences in fragmentation can be rationalized on the basis of electrostatic interactions.[23] This interpretation of the ECD data is also consistent with studies of cytochrome *c* ions complexed by crown ethers[24] in which it was shown that coordination of a lysine ammonium ion by 18-crown-6 inhibits the formation of intramolecular hydrogen bonds in cytochrome *c* ions, thereby shifting their conformer preferences.

Although there is very little empirical data on the processes associated with the structural transitions that occur during the final stages of electrosprayed solvent droplet evaporation, a number of studies have demonstrated that under mild ESI conditions biomolecular ions can retain memory of their solution structures.[25−28] Cryogenic IM-MS provided the first

Received: October 14, 2014
Revised: November 14, 2014

dx.doi.org/10.1021/jp5103687 | J. Phys. Chem. B XXXX, XXX, XXX−XXX

experimental data on the conformational changes that occur during the final stages of the dehydration process.[5,6,29] The data clearly showed that $[M + 3H]^{3+}$ ions of substance P (SP, an undecapeptide: RPKPQQFFGLM-NH_2) do not undergo significant conformational changes during the final steps of the dehydration process (i.e., loss of the last approximately 100 water molecules). Furthermore, the dominant conformer formed by dehydration under cold conditions is a kinetically trapped state, which is representative of a structural intermediate present during the conversion from solution to the gas-phase environment. Upon collisional heating, this conformer rearranges to the thermodynamically more stable gas-phase ion conformation. Molecular dynamics (MD) simulations revealed that the kinetically trapped conformer is stabilized through interactions between the charge sites (i.e., the N-terminus, the arginine (R) side chain guanidinium ion, and the ε-ammonium ion of the lysine (K) side chain) and polar residues, specifically the glutamines (Q) at positions 5 and 6 and possibly the phenylalanines (F) at positions 7 and 8. Moreover, simulated annealing studies showed that at increased temperatures these interactions are disrupted and that structural rearrangement of the collapsed-coil to an extended-coil conformation occurs. Here, we explore the effects of specific intramolecular interactions on conformer preferences and the stability of the kinetically trapped conformer of $[SP + 3H]^{3+}$ ions using specific amino acid mutations to eliminate salt bridge formation, specifically, substitution of Q^5/Q^6 and F^7/F^8 by alanine, and by altering the backbone orientation of the charge-carrying sites through proline (P) substitutions at positions 2, 4, and 9.

EXPERIMENTAL METHODS

Peptides and Ionization. The nomenclature, sequence, and purity of each peptide analyzed are listed in Table 1.

Table 1. Analyzed Peptides, Including Peptide Abbreviation, Sequence, and Percent Purity[a]

peptide	sequence	purity (%)
SP	RPKPQQFFGLM-NH_2	>95
RS	MLGFFQQPKPR-NH_2	>95
Q5A	RPKP<u>A</u>QFFGLM-NH_2	80
Q6A	RPKPQ<u>A</u>FFGLM-NH_2	84
Q5,6A	RPKP<u>AA</u>FFGLM-NH_2	83
F7,8A	RPKPQQ<u>AA</u>GLM-NH_2	84
Q5,6A F7,8A	RPKP<u>AAAA</u>GLM-NH_2	>95
P2A	R<u>A</u>KPQQFFGLM-NH_2	73
P4A	RPK<u>A</u>QQFFGLM-NH_2	85
P2,4A	R<u>A</u>K<u>A</u>QQFFGLM-NH_2	82
G9P	RPKPQQFF<u>P</u>LM-NH_2	75
P2,4A G9P	R<u>A</u>K<u>A</u>QQFF<u>P</u>LM-NH_2	90

[a]Amino acid residues that have been mutated with respect to substance P are underlined.

Collision cross sections (CCSs) for each peptide are listed in Table S1 of the Supporting Information (SI). SP and its reverse sequence (RS) were purchased from American Peptide (Sunnyvale, CA). Mutant peptides Q5A; Q6A; P2A; P4A; P2,4A; and G9P were purchased from Mocell (Shanghai, China). P2,4A G9P; Q5,6A F7,8A; Q5,6A; and F7,8A peptides were purchased from GenScript (Piscataway, NJ). Each lyophilized peptide was dissolved in 1 mL of water and stored at −20 °C. No further purification steps were performed. The impurities present in the samples were nonpeptidic and did not interfere with the IM-MS data (i.e., the CCS data is acquired on m/z selected $[SP + 3H]^{3+}$ ions). Aliquots of each stock solution were diluted 50:49:1 methanol:water:acetic acid to create ∼10 μM solutions. Samples were directly infused into the instrument through a pulled-tip fused silica emitter at 500 nL min^{-1}. The emitter was biased 1.8−2.0 kV relative to the heated capillary inlet to facilitate ESI.

Instrumentation and Data Acquisition. Arrival time distributions and mass spectra were collected on a home-built ion mobility-mass spectrometer (IM-MS) that has been described previously.[30] Briefly, the instrument consists of a periodic focusing ion funnel (PF IF), a 1.38 m-long periodic focusing ion mobility (PF IMS) drift tube, and an orthogonal acceleration time-of-flight mass analyzer. Ions are introduced into the instrument through a heated capillary inlet that is maintained at 70 °C to facilitate desolvation. The heated capillary is positioned orthogonal to the entrance of the PF IF to inhibit unwanted neutral contaminants from entering the mobility analyzer. Turning optics are used to direct ions from the flow of gas into the PF IF, where they are radially focused. A discrete packet of ions is pulsed into the drift tube by modulation of the potential on a ring electrode positioned at the back of the PF IF. Helium gas (99.999% purity) is added to the PF IF and PF IMS drift cell and yields pressures of ∼1.0 and 1.28 Torr, respectively. Collisional activation studies can be performed prior to IMS analysis by increasing the electric field in the PF IF from 23 to 38 V cm^{-1} $Torr^{-1}$. CCS values were obtained as described previously[31] using drift fields ranging from 19.2 to 14.7 V cm^{-1} $Torr^{-1}$. An IM-MS spectrum of $[SP + 3H]^{3+}$ ions was collected with isotopic mass resolution to determine the oligomer state of the distribution. The mass spectrum shows that the ion mobility peak profile corresponds to multiple conformations of monomeric SP ions (Figure S1, SI). All CCS values for mutant peptides have been corrected for the intrinsic size shift as described previously.[32,33]

Molecular Modeling. Annealing MD simulations were performed by the AMBER 11 suite. Custom residues were generated using GAUSSIAN 03 (HF/6-31+) and R.E.D. III charge fitting.[34] AMBER FF99SB force fields were used for the supported residues. Candidate structures generated by simulated annealing MDs undergo simulated heating and cooling cycles, which vary the temperature from 300 to 1000 K. Clustering statistical analysis was performed on the resulting structures as described previously.[35] The CCSs of the simulated structures were calculated using the MOBCAL software package.[36]

RESULTS AND DISCUSSION

Previous IM-MS studies have shown that $[SP + 3H]^{3+}$ ions formed by ESI can adopt two distinct conformations: a compact conformer denoted $\mathbf{A}_{SP}$ and an elongated conformer denoted $\mathbf{B}_{SP}$ (Figure 1). $\mathbf{B}_{SP}$ can also be formed by collisional activation of $\mathbf{A}_{SP}$.[5] These data are consistent with $\mathbf{A}_{SP}$ being representative of a kinetically trapped intermediate present upon complete desolvation. Kinetic trapping of $\mathbf{A}_{SP}$ is potentially facilitated through stabilizing interactions established between the localized charge sites present at the N-terminus and polar/aromatic residues along the peptide backbone; these effects are evaluated below.

The significance of the localized charge sites (N-terminus, R^1, and K^3) of the $[SP + 3H]^{3+}$ ions to the kinetic trapping of $\mathbf{A}_{SP}$ is shown by the analysis of the SP reverse-sequence (RS,

dx.doi.org/10.1021/jp5103687 | J. Phys. Chem. B XXXX, XXX, XXX−XXX

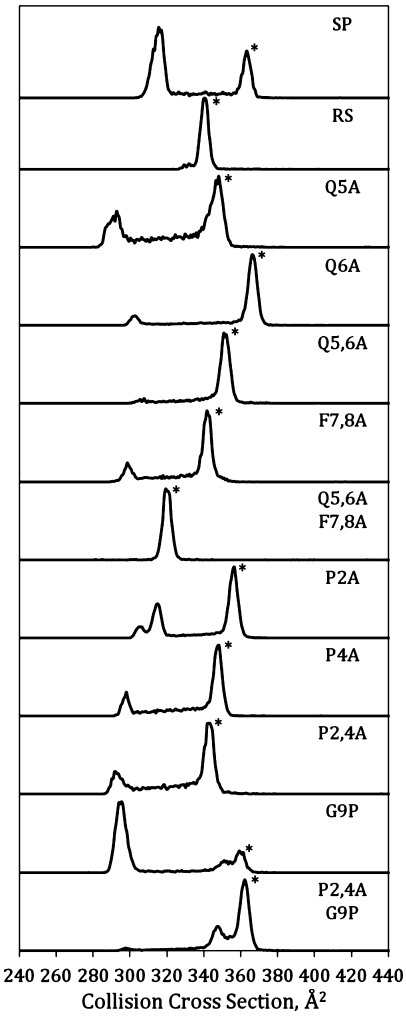

Figure 1. CCS profiles of SP and intrinsic size-corrected CCS profiles of SP mutant $[M + 3H]^{3+}$ ions. Shifts in the CCS profiles between SP and SP mutant ions arise from variations in ion packing efficiency that are not represented by the intrinsic size parameter shift. An asterisk denotes the elongated **B** conformer of each peptide ion. Assignment of the elongated conformer for peptide ions that have a single peak distribution was determined through collisional activation studies.

MLGFFQQPKPR-NH_2) peptide $[M + 3H]^{3+}$ ions, in which the charge sites of $[RS + 3H]^{3+}$ ions are located at the N-terminus, K^9, and R^{11}. The CCS profile for $[RS + 3H]^{3+}$ ions contains a single peak and a small, partially resolved, leading-edge peak (Figure 1) in which the dominant peak is assigned as the elongated conformer $\mathbf{B}_{RS}$. This assignment is based on the fact that collisional activation does not alter either the peak shape or peak width (Figure 3c), which would be expected if the distribution observed was representative of a kinetically trapped conformation. These data suggest that the localization of the charge sites in $[SP + 3H]^{3+}$ ions is imperative to the formation of stabilizing interactions and the subsequent stability of $\mathbf{A}_{SP}$. Thus, separating the charge sites on opposite ends of the peptide ion promotes elongation of the peptide backbone.

The following sections describe experiments aimed at identifying specific sites of intramolecular interactions and the importance of each site to the collective stabilization of $\mathbf{A}_{SP}$. Here, we employ amino acid mutations of native residues to alanine to eliminate potential interaction sites while minimizing the steric effects of more bulky side chains using amino acids such as valine, leucine, or isoleucine. IM-MS is then used to measure changes in the conformer preferences of the modified peptide ions.[37−42] The CCS profiles of SP and SP mutant $[M + 3H]^{3+}$ ions shown in Figure 1 illustrate two effects of the amino acid mutations: (1) the CCS values for each mutant are shifted due to an overall change in the size (shape) of the ion, and (2) the relative abundances and peak widths of the kinetically trapped compact **A** and energetically preferred elongated **B** conformers are perturbed relative to that of $\mathbf{A}_{SP}$ and $\mathbf{B}_{SP}$.

Intramolecular Interactions. The CCS profiles shown in Figure 1 are corrected for differences in the intrinsic size parameters of the amino acids, but it should be noted that the size-corrected CCS values do not align exactly with those for SP. The data illustrate that amino acid mutations may alter both intramolecular interactions, as will be discussed further, as well as ion-packing efficiency owing to steric effects of the side chains. Thus, all effects of amino acid mutations on CCSs are not accounted for by the intrinsic size correction and result in misalignment of these values for SP mutant peptide ions with respect to those of SP. Nevertheless, the structural conversion of conformer **A** to **B** is maintained for all mutant ions, suggesting that kinetic trapping is still occurring for the mutant peptide ions. Additionally, by altering the formation of the stabilizing interactions, these mutations provide a qualitative depiction of the importance of intramolecular interactions to kinetic trapping.

The CCS profiles for mutant Q5A and Q6A $[M + 3H]^{3+}$ ions are composed of two distinct peaks consistent with $\mathbf{A}_{SP}$ and $\mathbf{B}_{SP}$, but the relative abundances of $\mathbf{A}_{Q5A}$ and $\mathbf{A}_{Q6A}$ are reduced compared to those of $\mathbf{A}_{SP}$. Changes in the relative abundances of conformer **A** for these mutant ions support the argument that conformer **A** is stabilized by intramolecular interactions involving Q^5 and Q^6. Moreover, the peak width of $\mathbf{A}_{Q6A}$ is reduced compared to that of $\mathbf{A}_{SP}$, which is consistent with a decrease in the conformational heterogeneity of conformer **A**. Interestingly, although the CCS profile of $[Q5A + 3H]^{3+}$ shows a decrease in the relative abundance of conformer **A**, the peak width appears to be somewhat broader than that for $\mathbf{A}_{SP}$. In fact, two compact conformations (denoted $\mathbf{A}_{1,Q5A}$ and $\mathbf{A}_{2,Q5A}$) are partially resolved at reduced drift fields, whereas $\mathbf{A}_{SP}$ remains an unresolved distribution of conformers (Figure S2, SI). At higher drift fields, both $\mathbf{A}_{1,Q5A}$ and $\mathbf{A}_{2,Q5A}$ undergo structural conversion during mobility analysis to adopt the elongated conformation, which leads to comparable peak widths for $\mathbf{A}_{SP}$ and $\mathbf{A}_{Q5A}$. Nevertheless, these data show that elimination of a single interaction site destabilizes specific conformations within distribution **A**, which leads to a reduction in the structural heterogeneity of the distribution. Furthermore, as shown by comparable peak widths, conformer **B** remains largely unaltered by the mutations. The conversion of conformer **A** to **B** upon collisional activation is also maintained with the elimination of single intramolecular interaction sites (Figure S3, SI), suggesting that the adoption of conformer **B** is independent of the interactions involving Q^5 or Q^6.

The stabilizing contributions established through interactions involving either Q^5 or Q^6 are examined with the Q5,6A mutant. The CCS profile of $[Q5,6A + 3H]^{3+}$ shows a dominant $\mathbf{B}_{Q5,6A}$ conformer population (352 $Å^2$) and an $\mathbf{A}_{Q5,6A}$ conformer (~295 $Å^2$) that has a relative abundance of <5%. These data suggest that interactions between the charge sites and Q^5/Q^6 provide the greatest stability to the kinetically trapped conformation. Molecular modeling data for SP show that $\mathbf{A}_{SP}$ is stabilized by

dx.doi.org/10.1021/jp5103687 | J. Phys. Chem. B XXXX, XXX, XXX−XXX

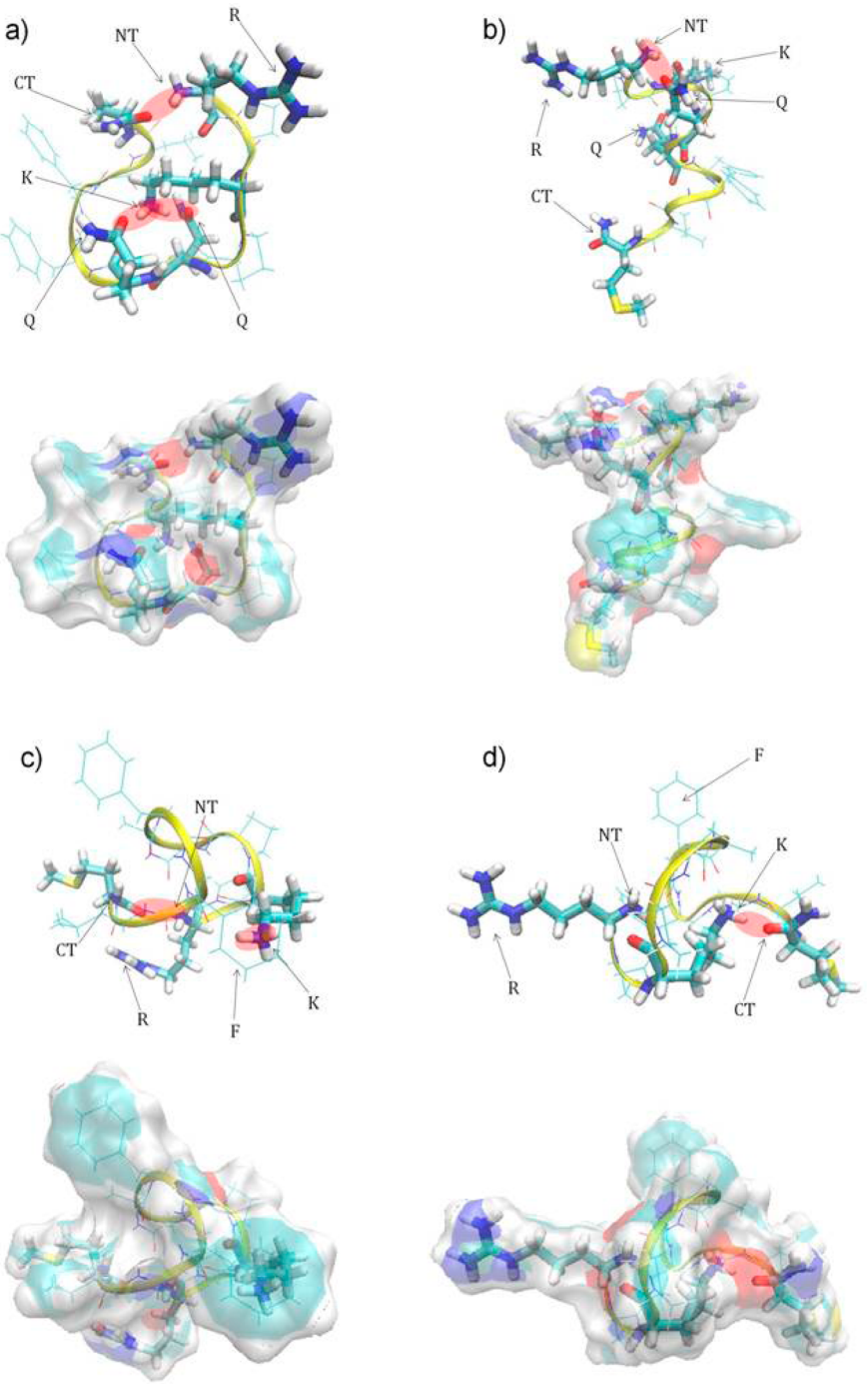

Figure 2. Best-fit structures of (a) $\mathbf{A}_{SP}$, (b) $\mathbf{B}_{SP}$, (c) $\mathbf{A}_{Q5,6A}$, and (d) $\mathbf{B}_{Q5,6A}$ as determined by molecular modeling. $\mathbf{A}_{SP}$ is stabilized by interactions between K^3 and Q^5/Q^6 and the N-terminus (NT) with the C-terminus (CT). The K^3 and Q^5/Q^6 interactions are absent for $\mathbf{A}_{Q5,6A}$, which is due to the aliphatic nature of A^5/A^6; however, $\mathbf{A}_{Q5,6A}$ is stabilized by interactions between the NT and the CT and K^3 with the F residues. The elongated conformer for both SP and Q5,6A suggests that elongation originates from a disruption of intramolecular interactions and a subsequent outward projection of R^1 and/or K^3 on the basis of Coulombic repulsion. Intramolecular interactions are highlighted in red. Clustering was performed on uncorrected CCS values for the Q5,6A mutant. A space-filling model is shown below each best-fit structure.

interactions between the charge sites and Q^5/Q^6 (Figure 2). Conversely, representative structures of $\mathbf{A}_{Q5,6A}$ do not show any interaction with A^5/A^6 owing to the aliphatic nature of alanine; however, $\mathbf{A}_{Q5,6A}$ is stabilized by interactions between the charge sites and the peptide backbone as well as interactions involving F^7 and F^8. It is interesting to note the similarities between $\mathbf{B}_{SP}$ and $\mathbf{B}_{Q5,6A}$ revealed by the modeling data (Figure 2). It appears that elongation of SP and Q5,6A arises from a projection of R^1 and/or K^3 outward upon disruption of intramolecular interactions involving these residues, which suggests that conformer **B** for SP and Q5,6A are quite similar in structure. These modeling data are consistent with the hypothesis that interactions between the charge sites and Q^5/Q^6 afford the greatest stabilization to conformer **A**, and that through the elimination of these residues, minor interactions involving the

dx.doi.org/10.1021/jp5103687 | J. Phys. Chem. B XXXX, XXX, XXX−XXX

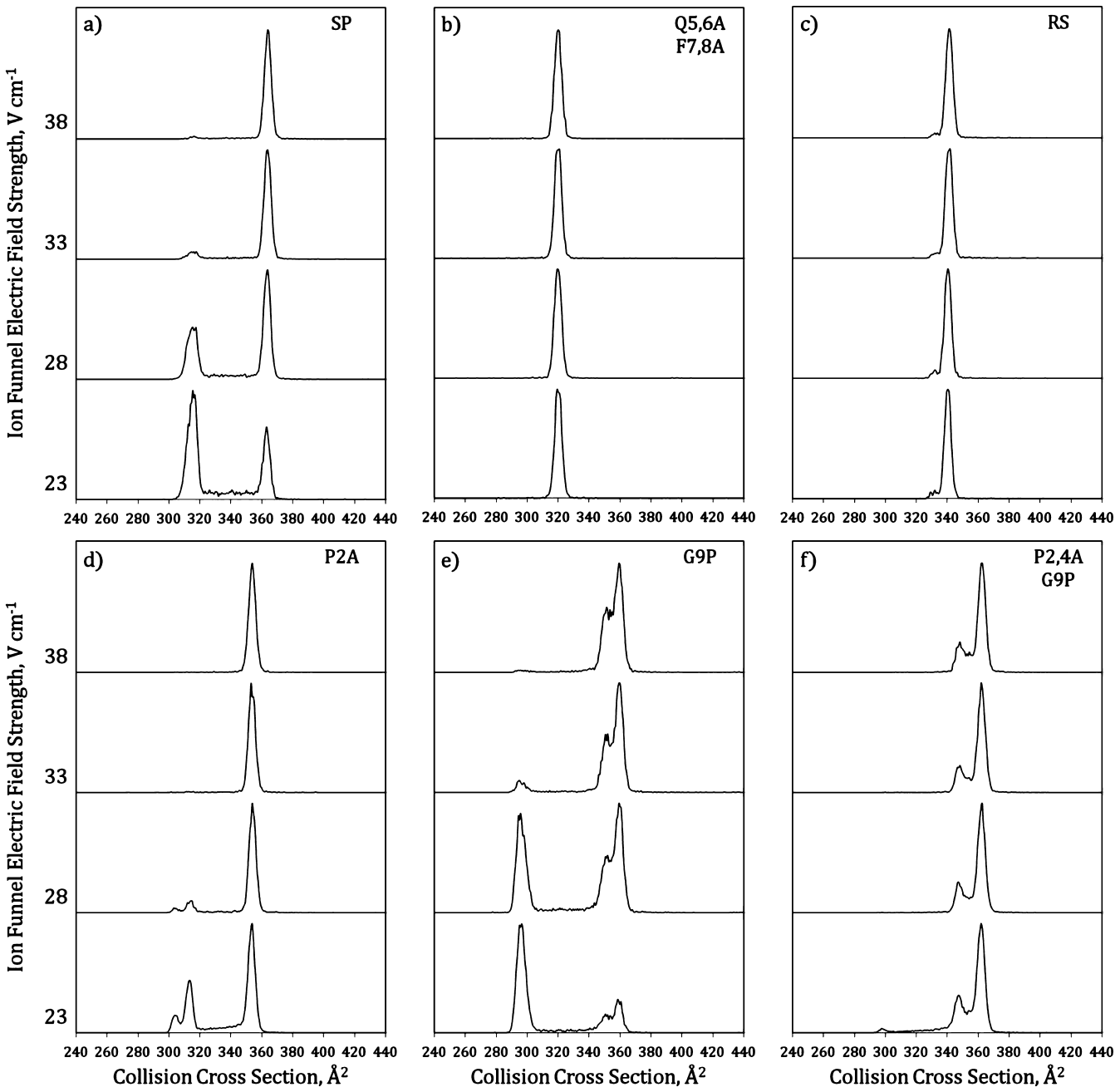

Figure 3. CCS profiles of (a) SP, (b) Q5,6A F7,8A, (c) RS, (d) P2A, (e) G9P, and (f) P2,4A G9P as a function of axial electric field in the PF IF. In the lowest electric field (23 V cm^{-1}), the kinetically trapped conformer is seen for SP, P2A, G9P, and P2,4A G9P. When the electric field is increased, these kinetically trapped conformers undergo structural rearrangement to form the elongated conformer. For Q5,6A F7,8A and RS peptide ions, the absence of any structural variation indicates that the elongated conformation is the distribution observed at 23 V cm^{-1}.

peptide backbone and/or the F^7 and F^8 residues provide stability to this conformation.

Possible stabilizing contributions established through π-cation interactions with F^7 and F^8 are examined with the F7,8A mutant. The CCS profile of F7,8A exhibits the characteristic **A** and **B** conformers (Figure 1). The peak width of $\mathbf{A}_{F7,8A}$ (299 $Å^2$) is reduced relative to that of $\mathbf{A}_{SP}$, and the relative abundance with respect to $\mathbf{B}_{F7,8A}$ (342 $Å^2$) is ~15%. Similar to the single-point mutations previously discussed, the decrease in peak width for $\mathbf{A}_{F7,8A}$ is indicative of an elimination of conformers that are stabilized by π-cation interactions involving F^7 and F^8. Reduction in the relative abundance of $\mathbf{A}_{F7,8A}$ is comparable to the reduction observed for single Q mutations, suggesting that interactions between the charge sites and F^7/F^8 provide less stability than those established with Q^5/Q^6, a result that is consistent with the MD simulations. Additionally, the CCS profile of F7,8A is shifted to a lower CCS with respect to that of SP. MD simulations of both SP and Q5,6A show that the phenyl side chains of F^7 and F^8 are typically on the exterior of the ion in the **A** and **B** conformations. Thus, the F7,8A mutation eliminates the bulky phenyl side chains and causes the shift to lower CCS values on the basis of decreased steric bulkiness of the methyl side chains of A^7 and A^8. The observed shift to lower CCS values further supports the hypothesis that changes to the steric bulk of side chains can affect the packing

dx.doi.org/10.1021/jp5103687 | J. Phys. Chem. B XXXX, XXX, XXX–XXX

Table 2. Possible Cis/Trans Isomer Distributions for the 2nd, 4th, and 9th Residue Positions[a]

	isomer distribution			conformer distribution			
				A peaks		B peaks	
peptide name	2nd residue	4th residue	9th residue	expected	observed	expected	observed
P2A	trans	cis/trans	trans	2	2	1	1
P4A	cis/trans	trans	trans	2	2[b]	1	1
P2,4A	trans	trans	trans	1	1	1	1
G9P	cis/trans	cis/trans	cis/trans	1[c]	1	2	2
P2,4A G9P	trans	trans	cis/trans	1	1	2	2

[a]For ions with a cis/trans isomer distribution in the 2nd and 4th residues, the expected number of **A** peaks is two. When the cis/trans isomer distribution is located in the 9th residue position, **B** is split into two peaks [b]Two peaks for **A** were observed at reduced PF IMS drift cell fields. [c]One peak is expected for **A** on the basis of the native sequence of amino acids 1−8.

efficiency of the ions and are not accounted for by the inclusion of an intrinsic size parameter shift.

A search for additional intramolecular interactions was performed by examining the mutant Q5,6A F7,8A, which eliminates all interactions with Q and F residues. The CCS profile for the Q5,6A F7,8A mutant is composed of a single peak, but it is not obvious whether this is conformer **A** or **B**. Collisional activation of $\mathbf{A}_{SP}$ yields $\mathbf{B}_{SP}$ (Figure 3a); thus, it is expected that a similar result would be obtained for $\mathbf{A}_{Q5,6A\ F7,8A}$ (Figure 3b). However, collisional activation does not change the CCS profile, suggesting that the observed peak is conformer **B**. Additionally, CCS correction based on individual mutations shows that the CCS for this mutant is consistent with the value expected for the elongated conformation.[43] Lastly, when employing instrument conditions that minimize collisional activation, a distribution of less than 20% relative abundance is observed at smaller CCS values in addition to the distribution observed at 320 Å^2 (Figure S4, SI). Thus, the single peak is representative of the elongated conformation $\mathbf{B}_{Q5,6AF7,8A}$ (320 Å^2), and the elimination of Q^5/Q^6 and F^7/F^8 decreases the stability of $\mathbf{A}_{Q5,6AF7,8A}$ to the point that it is not observed under these experimental conditions.

The Proline Effect. The charge sites (i.e., N-terminus, arginine, and lysine side chains) of $[SP + 3H]^{3+}$ ions are separated by prolines (P) at positions 2 and 4, and it is plausible that cis and trans conversions at these sites may provide a mechanism by which to increase charge separation. Although the trans configuration of most amino acids is thermodynamically favored by ∼3.5 kJ mol^{-1},[44] the trans isomer of proline is energetically favored by as little as ∼0.5 kJ mol^{-1}.[43,45−47] Pierson et al. showed that proline to alanine mutations, which eliminate the cis isomer, depopulated specific conformers of bradykinin $[M + 3H]^{3+}$ ions.[43] In fact, SP is similar to bradykinin in that the prolines are located near the charge sites for both peptides. Because of the proximity of the P^2 and P^4 residues to the charge sites of SP, it is of interest to consider the implications of the cis and trans isomers of P^2 and P^4 with regard to the formation of stabilizing intramolecular interactions as described above. The CCS profile of P2A contains three distinct peaks (Figure 1), and the relative abundances of the peaks labeled $\mathbf{A}_{1,P2A}$ (303 Å^2) and $\mathbf{A}_{2,P2A}$ (315 Å^2) are smaller than that of $\mathbf{A}_{SP}$, which would suggest that the cis-P^2 isomer, which was eliminated upon mutation, affords stabilization of $\mathbf{A}_{SP}$. Note also that the peak widths for both $\mathbf{A}_{1,P2A}$ and $\mathbf{A}_{2,P2A}$ are decreased relative to that of $\mathbf{A}_{SP}$, and collisional activation does not change the ratio of $\mathbf{A}_{1,P2A}$ to $\mathbf{A}_{2,P2A}$ (Figure 3d), indicating that both conformers are stabilized by intramolecular interactions. The $\mathbf{A}_{1,P2A}$ and $\mathbf{A}_{2,P2A}$ conformers may correspond to cis and trans configurations at P^4; this possibility was tested by examining additional SP mutants. Predicted residue-specific isomer distributions and possible cis/trans isomers for proline to alanine mutant peptide ions are listed in Table 2.

Mutant P4A replaces the possible cis/trans isomers at P^4 with a trans-only isomer but allows P^2 to adopt either a cis or trans isomer. Assuming the P4A mutant behaves similarly to the P2A mutant, the CCS profile for conformer **A** of P4A should consist of two peaks; however, the CCS profile contains a single peak for conformer $\mathbf{A}_{P4A}$ (300 Å^2, Figure 1). This result clearly shows that P^2 and P^4 exert very different effects on the conformation of $[SP + 3H]^{3+}$ ions. Although the orientation of P^4 can influence the projection of three amino acid residues, including all three charge sites, the isomer preference of P^2 affects the orientation of only the R^1 side chain. Thus, the difference in CCS resulting from different orientations of the R^1 side chain originating from the cis and trans isomers of P^2 may not be resolvable under current experimental conditions. Consistent with this, at higher mobility resolutions, the CCS profiles for P4A are comprised of two peaks for conformers for **A**, $\mathbf{A}_{1,P4A}$, and $\mathbf{A}_{2,P4A}$, which are partially resolved (Figure S5, SI). Interestingly, the ratio of $\mathbf{A}_{1,P4A}$ to $\mathbf{A}_{2,P4A}$ is unique compared to that observed for P2A. The variation in this ratio of $\mathbf{A}_1$ and $\mathbf{A}_2$ for P2A and P4A may result from electrostatic interactions between the guanidinium ion and P^2. Interactions between proline and the guanidinium ion have been previously shown to influence the activity of enzymes, suggesting that the presence of arginine can play an important role in determining the cis/trans isomer distribution of the neighboring proline residue.[48] Nevertheless, the reduction of the relative abundance of conformer **A** and the decrease in peak width observed for $\mathbf{A}_{P4A}$ are consistent with the elimination of stabilizing interactions facilitated by the cis isomer of P^4.

The P2,4A mutant should produce a single distribution for conformer **A** owing to the elimination of cis isomers (Table 2), and indeed, the CCS profile contains a single distribution for $\mathbf{A}_{P2,4A}$ (293 Å^2). There is also a reduction in the relative abundance of $\mathbf{A}_{P2,4A}$ and a decrease in the peak width (Figure 1). The resulting changes in conformer heterogeneity by P2A, P4A, and P2,4A clearly illustrate the effects of cis/trans isomers on the conformer population. Moreover, the effect of these mutations on the relative abundances of conformer **A** suggests that changes in the backbone orientation also affect intramolecular charge solvation.

Inducing the Cis/Trans Effect within Conformer B. The mutant peptide ions analyzed thus far have little to no influence on the conformational preference of **B**, which is because the mutations were isolated to residues that establish stabilizing intramolecular interactions (i.e., R^1 through F^8). Mutant G9P

dx.doi.org/10.1021/jp5103687 | J. Phys. Chem. B XXXX, XXX, XXX−XXX

introduces proline near the C-terminus and induces cis/trans heterogeneity, resulting in changes to the CCS profile. Namely, two distributions are detected for conformer **B** (Figure 1), $\mathbf{B}_{1,G9P}$ (352 Å^2) and $\mathbf{B}_{2,G9P}$ (360 Å^2), with each distribution being present in less than 20% relative abundance. Interestingly, $\mathbf{A}_{G9P}$ (295 Å^2) is comparable to $\mathbf{A}_{SP}$ as shown by each conformer being present in 100% relative abundance and having similar peak widths. These observations indicate that the G9P mutation does not negate the intramolecular interactions that provide stability to $\mathbf{A}_{SP}$. Reduction in the relative abundance of $\mathbf{B}_{G9P}$ compared to that of $\mathbf{B}_{SP}$ arises from the mutation partitioning the extended conformation into two conformer populations. Splitting of conformer **B** by the G9P mutation suggests that cis/trans isomer heterogeneity of the G9P conformer population has been introduced, consistent with the predicted distribution (Table 2).

If all aforementioned hypotheses are correct, the P2,4A G9P mutant should exhibit a reduction in the relative abundance of the compact conformation by eliminating cis dependent interactions and show two conformers for $\mathbf{B}_{P2,4A\ G9P}$ owing to cis/trans heterogeneity. The CCS profile of P2,4A G9P shows a compact conformer of $\mathbf{A}_{P2,4A\ G9P}$ (298 Å^2) that is less than 10% relative abundance and an extended conformation comprised of two partially resolved distributions: $\mathbf{B}_{1,P2,4A\ G9P}$ (347 Å^2) and $\mathbf{B}_{2,P2,4A\ G9P}$ (362 Å^2, Figure 1). Further reduction of $\mathbf{A}_{P2,4A\ G9P}$ compared to that of $\mathbf{A}_{P2,4A}$ suggests that the cis isomer in the 9th residue position destabilizes the minor interactions associated with the C-terminus. Nevertheless, these data confirm the aforementioned hypotheses by demonstrating that the combination of destabilization and isomer heterogeneity inclusion can be achieved through select mutations.

CONCLUSIONS

Specific mutations of SP were utilized to examine the factors that influence kinetic trapping of $\mathbf{A}_{SP}$. The stabilizing effects afforded by the localization of the charge sites of the $[SP + 3H]^{3+}$ ion were examined by analysis of the $[M + 3H]^{3+}$ ion of the reverse sequence peptide. Because of the separation of the charge sites, the CCS profile of $[RS + 3H]^{3+}$ showed a single distribution that was assigned to $\mathbf{B}_{RS}$, which suggested that formation of the intramolecular interactions responsible for kinetic trapping of $\mathbf{A}_{SP}$ is dependent on charge site location. Furthermore, amino acid mutations of native SP were utilized to determine possible interaction sites. Upon elimination of single Q residues, the relative abundance of the kinetically trapped, compact conformer **A** population was reduced to ~20%, and the peak width was decreased on the basis of reduced structural heterogeneity. Double residue mutations of Q^5/Q^6 and F^7/F^8 showed that interactions with Q^5/Q^6 are critical for the formation of conformer **A**, whereas interactions with F^7/F^8 provided stability to a lesser extent. Upon elimination of all Q/F residues, conformer **A** was completely destabilized, and the energetically preferred, gas-phase conformer **B** was favored. Thus, intramolecular interactions attributed to Q^5/Q^6 and F^7/F^8 provide a means of kinetically trapping conformer **A**. Moreover, these interactions delocalize the charges present on the $[M + 3H]^{3+}$ ion; upon elimination of these interactions, there is an increase in Coulombic repulsion and reduction in the gas-phase basicity of the charge sites. The combination of these effects may favor proton transfer to the amide C-terminal group, which is facilitated through interactions involving the N- and C-termini. Collectively, these stabilizing interactions are critical to the preservation of the kinetically trapped species in the gas phase.

The impact of cis and trans isomers of proline on the formation of intramolecular interactions was explored through mutations. Two proline residues, P^2 and P^4, occur in the N-terminal region of SP and are in close proximity to the charge sites. Upon mutation of these residues to effectively eliminate the cis isomer, the conformational heterogeneity of conformer **A** was reduced, suggesting that the cis isomer facilitates the formation of certain interactions. Additionally, upon elimination of the cis isomer at P^2 or P^4, conformer **A** was resolved into two distinct distributions that could have originated from the cis and trans isomers of the remaining P residue. To investigate the capacity for inducing conformational splitting between cis and trans isomers, proline was mutated in the C-terminal region of SP. This mutation showed no impact on conformer **A** but introduced an additional population for conformer **B**, which is consistent with cis/trans isomer heterogeneity. The combined effects of destabilization and cis/trans heterogeneity induction were explored using the mutation P2,4A G9P. IM-MS analysis of this mutant confirmed that the effects could be combined (i.e., conformer **A** was destabilized, and conformer **B** was split into two peaks, indicative of the presence of cis and trans populations). Collectively, these results show that the isomeric preferences of proline can directly impact the formation of stabilizing interactions as well as alter the conformational preferences of conformer **B**.

ASSOCIATED CONTENT

Supporting Information

Collision cross sections, additional arrival time distributions, and collisional activation studies. This material is available free of charge via the Internet at http://pubs.acs.org.

AUTHOR INFORMATION

Corresponding Author

*E-mail: russell@mail.chem.tamu.edu. Phone: (979) 845-3345.

Notes

The authors declare no competing financial interest.

ACKNOWLEDGMENTS

The authors acknowledge Will Seward, Carl Johnson, and Ron Page of the Chemistry Department's Machine Shop for fabrication of all custom instrumentation, and Greg Matthijetz of the Laboratory for Biological Mass Spectrometry for his vast electronics expertise. This research was supported by the U.S. Department of Energy, Division of Chemical Sciences (BES DE-FG02-04ER15520). Funding for the simulations was provided by the National Science Foundation (Grant CHE-0541587). The authors also acknowledge DoYong Kim, Dr. Lisa Perez, and the Laboratory for Molecular Simulations for their contributions to this work.

REFERENCES

(1) Nagornova, N. S.; Rizzo, T. R.; Boyarkin, O. V. Interplay of Intra- and Intermolecular H-Bonding in a Progressively Solvated Macrocyclic Peptide. *Science* **2012**, *336*, 320−323.

(2) Garand, E.; Kamrath, M. Z.; Jordan, P. A.; Wolk, A. B.; Leavitt, C. M.; McCoy, A. B.; Miller, S. J.; Johnson, M. A. Determination of Noncovalent Docking by Infrared Spectroscopy of Cold Gas-Phase Complexes. *Science* **2012**, *335*, 694−698.

(3) Prell, J. S.; Correra, T. C.; Chang, T. M.; Biles, J. A.; Williams, E. R. Entropy Drives an Attached Water Molecule from the C- to N-Terminus on Protonated Proline. *J. Am. Chem. Soc.* **2010**, *132*, 14733−14735.
(4) Prell, J. S.; Chang, T. M.; O'Brien, J. T.; Williams, E. R. Hydration Isomers of Protonated Phenylalanine and Derivatives: Relative Stabilities from Infrared Photodissociation. *J. Am. Chem. Soc.* **2010**, *132*, 7811−7819.
(5) Silveira, J. A.; Fort, K. L.; Kim, D.; Servage, K. A.; Pierson, N. A.; Clemmer, D. E.; Russell, D. H. From Solution to the Gas Phase: Stepwise Dehydration and Kinetic Trapping of Substance P Reveals the Origin of Peptide Conformations. *J. Am. Chem. Soc.* **2013**, *135*, 19147−19153.
(6) Silveira, J. A.; Servage, K. A.; Gamage, C. M.; Russell, D. H. Cryogenic Ion Mobility-Mass Spectrometry Captures Hydrated Ions Produced During Electrospray Ionization. *J. Phys. Chem. A* **2013**, *117*, 953−961.
(7) Breuker, K.; Brueschweiler, S.; Tollinger, M. Electrostatic Stabilization of a Native Protein Structure in the Gas Phase. *Angew. Chem., Int. Ed.* **2011**, *50*, 873−877.
(8) Breuker, K.; McLafferty, F. W. Stepwise Evolution of Protein Native Structure with Electrospray into the Gas Phase, 10^{-12} to 10^{2} s. *Proc. Natl. Acad. Sci. U.S.A.* **2008**, *105*, 18145−18152.
(9) Papadopoulos, G.; Svendsen, A.; Boyarkin, O. V.; Rizzo, T. R. Conformational Distribution of Bradykinin $[BK + 2H]^{2+}$ Revealed by Cold Ion Spectroscopy Coupled with FAIMS. *J. Am. Soc. Mass Spectrom.* **2012**, *23*, 1173−1181.
(10) Papadopoulos, G.; Svendsen, A.; Boyarkin, O. V.; Rizzo, T. R. Spectroscopy of Mobility-Selected Biomolecular Ions. *Faraday Discuss.* **2011**, *150*, 243−255.
(11) Deng, Z.; Thontasen, N.; Malinowski, N.; Rinke, G.; Harnau, L.; Rauschenbach, S.; Kern, K. A Close Look at Proteins: Submolecular Resolution of Two- and Three-Dimensionally Folded Cytochrome c at Surfaces. *Nano Lett.* **2012**, *12*, 2452−2458.
(12) Wyttenbach, T.; Bowers, M. T. Structural Stability from Solution to the Gas Phase: Native Solution Structure of Ubiquitin Survives Analysis in a Solvent-Free Ion Mobility-Mass Spectrometry Environment. *J. Phys. Chem. B* **2011**, *115*, 12266−12275.
(13) Skinner, O. S.; McLafferty, F. W.; Breuker, K. How Ubiquitin Unfolds after Transfer into the Gas Phase. *J. Am. Soc. Mass Spectrom.* **2012**, *23*, 1011−1014.
(14) van der Spoel, D.; Marklund, E. G.; Larsson, D. S. D.; Caleman, C. Proteins, Lipids, and Water in the Gas Phase. *Macromol. Biosci.* **2011**, *11*, 50−59.
(15) Pierson, N. A.; Valentine, S. J.; Clemmer, D. E. Evidence for a Quasi-Equilibrium Distribution of States for Bradykinin $[M + 3H]^{3+}$ Ions in the Gas Phase. *J. Phys. Chem. B* **2010**, *114*, 7777−7783.
(16) Shi, H. L.; Pierson, N. A.; Valentine, S. J.; Clemmer, D. E. Conformation Types of Ubiquitin $[M + 8H]^{8+}$ Ions from Water:-Methanol Solutions: Evidence for the N and A States in Aqueous Solution. *J. Phys. Chem. B* **2012**, *116*, 3344−3352.
(17) Pierson, N. A.; Chen, L.; Valentine, S. J.; Russell, D. H.; Clemmer, D. E. Number of Solution States of Bradykinin from Ion Mobility and Mass Spectrometry Measurements. *J. Am. Chem. Soc.* **2011**, *133*, 13810−13813.
(18) Ruotolo, B. T.; Giles, K.; Campuzano, I.; Sandercock, A. M.; Bateman, R. H.; Robinson, C. V. Evidence for Macromolecular Protein Rings in the Absence of Bulk Water. *Science* **2005**, *310*, 1658−1661.
(19) Barrera, N. P.; Di Bartolo, N.; Booth, P. J.; Robinson, C. V. Micelles Protect Membrane Complexes from Solution to Vacuum. *Science* **2008**, *321*, 243−246.
(20) van den Heuvel, R. H. H.; Heck, A. J. R. Native Protein Mass Spectrometry: From Intact Oligomers to Functional Machineries. *Curr. Opin. Chem. Biol.* **2004**, *8*, 519−526.
(21) Myung, S.; Badman, E. R.; Lee, Y. J.; Clemmer, D. E. Structural Transitions of Electrosprayed Ubiquitin Ions Stored in an Ion Trap over ∼10 ms to 30 s. *J. Phys. Chem. A* **2002**, *106*, 9976−9982.
(22) Skinner, O. S.; Breuker, K.; McLafferty, F. W. Charge Site Mass Spectra: Conformation-Sensitive Components of the Electron Capture Dissociation Spectrum of a Protein. *J. Am. Soc. Mass Spectrom.* **2013**, *24*, 807−810.
(23) Schennach, M.; Breuker, K. Proteins with Highly Similar Native Folds can show Vastly Dissimilar Folding Behavior when Desolvated. *Angew. Chem., Int. Ed.* **2014**, *53*, 164−168.
(24) Warnke, S.; von Helden, G.; Pagel, K. Protein Structure in the Gas Phase: The Influence of Side-Chain Microsolvation. *J. Am. Chem. Soc.* **2013**, *135*, 1177−1180.
(25) Morsa, D.; Gabelica, V.; De Pauw, E. Effective Temperature of Ions in Traveling Wave Ion Mobility Spectrometry. *Anal. Chem.* **2011**, *83*, 5775−5782.
(26) Merenbloom, S. I.; Flick, T. G.; Williams, E. R. How Hot Are Your Ions in TWAVE Ion Mobility Spectrometry? *J. Am. Soc. Mass Spectrom.* **2012**, *23*, 553−562.
(27) Zhou, M.; Dagan, S.; Wysocki, V. H. Protein Subunits Released by Surface Collisions of Noncovalent Complexes: Nativelike Compact Structures Revealed by Ion Mobility Mass Spectrometry. *Angew. Chem., Int. Ed.* **2012**, *51*, 4336−4339.
(28) Ruotolo, B. T.; Benesch, J. L. P.; Sandercock, A. M.; Hyung, S.-J.; Robinson, C. V. Ion Mobility-Mass Spectrometry Analysis of Large Protein Complexes. *Nat. Protoc.* **2008**, *3*, 1139−1152.
(29) Servage, K. A.; Silveira, J. A.; Fort, K. L.; Russell, D. H. Evolution of Hydrogen-Bond Networks in Protonated Water Clusters $H^+(H_2O)_n$ (n = 1 to 120) Studied by Cryogenic Ion Mobility-Mass Spectrometry. *J. Phys. Chem. Lett.* **2014**, *5*, 1825−1830.
(30) Fort, K. L.; Silveira, J. A.; Russell, D. H. The Periodic Focusing Ion Funnel: Theory, Design, and Experimental Characterization by High-Resolution Ion Mobility-Mass Spectrometry. *Anal. Chem.* **2013**, *85*, 9543−9548.
(31) Silveira, J. A.; Jeon, J.; Gamage, C. M.; Pai, P. J.; Fort, K. L.; Russell, D. H. Damping Factor Links Periodic Focusing and Uniform Field Ion Mobility for Accurate Determination of Collision Cross Sections. *Anal. Chem.* **2012**, *84*, 2818−2824.
(32) Valentine, S. J.; Counterman, A. E.; Clemmer, D. E. A Database of 660 Peptide Ion Cross Sections: Use of Intrinsic Size Parameters for Bona Fide Predictions of Cross Sections. *J. Am. Soc. Mass Spectrom.* **1999**, *10*, 1188−1211.
(33) Srebalus Barnes, C. A.; Clemmer, D. E. Assessing Intrinsic Side Chain Interactions between i and i + 4 Residues in Solvent-Free Peptides: A Combinatorial Gas-Phase Approach. *J. Phys. Chem. A* **2003**, *107*, 10566−10579.
(34) Dupradeau, F.-Y.; Pigache, A.; Zaffran, T.; Savineau, C.; Lelong, R.; Grivel, N.; Lelong, D.; Rosanski, W.; Cieplak, P. The R.E.D. Tools: Advances in RESP and ESP Charge Derivation and Force Field Library Building. *Phys. Chem. Chem. Phys.* **2010**, *12*, 7821−7839.
(35) Chen, L. X.; Shao, Q.; Gao, Y. Q.; Russell, D. H. Molecular Dynamics and Ion Mobility Spectrometry Study of Model β-Hairpin Peptide, Trpzip1. *J. Phys. Chem. A* **2011**, *115*, 4427−4435.
(36) Jarrold, M. F. http://www.indiana.edu/~nano/software.html.
(37) Hacke, M.; Gruber, T.; Schulenburg, C.; Balbach, J.; Arnold, U. Consequences of Proline-to-Alanine Substitutions for the Stability and Refolding of Onconase. *FEBS J.* **2013**, *280*, 4454−4462.
(38) Kotarba, A. E.; Aucoin, D.; Hoos, M. D.; Smith, S. O.; Van Nostrand, W. E. Fine Mapping of the Amyloid β-Protein Binding Site on Myelin Basic Protein. *Biochemistry* **2013**, *52*, 2565−2573.
(39) Coffa, S.; Breitman, M.; Spiller, B. W.; Gurevich, V. V. A Single Mutation in Arrestin-2 Prevents ERK1/2 Activation by Reducing c-Raf1 Binding. *Biochemistry* **2011**, *50*, 6951−6958.
(40) Lowman, H. B.; Bass, S. H.; Simpson, N.; Wells, J. A. Selecting High-Affinity Binding Proteins by Monovalent Phage Display. *Biochemistry* **1991**, *30*, 10832−10838.
(41) Cunningham, B. C.; Henner, D. J.; Wells, J. A. Engineering Human Prolactin to Bind to the Human Growth Hormone Receptor. *Science* **1990**, *247*, 1461−1465.
(42) Cunningham, B. C.; Wells, J. A. High-Resolution Epitope Mapping of hGH-receptor Interactions by Alanine-Scanning Mutagenesis. *Science* **1989**, *244*, 1081−1085.

(43) Pierson, N. A.; Chen, L.; Russell, D. H.; Clemmer, D. E. Cis−Trans Isomerizations of Proline Residues are Key to Bradykinin Conformations. *J. Am. Chem. Soc.* **2013**, *135*, 3186−3192.
(44) Ramachandran, G. N.; Sasisekharan, V. Conformation of Polypeptides and Proteins. *Adv. Protein Chem.* **1968**, *23*, 283−438.
(45) Stewart, D. E.; Sarkar, A.; Wampler, J. E. Occurrence and Role of Cis Peptide Bonds in Protein Structures. *J. Mol. Biol.* **1990**, *214*, 253−260.
(46) Dodge, R. W.; Scheraga, H. A. Folding and Unfolding Kinetics of the Proline-to-Alanine Mutants of Bovine Pancreatic Ribonuclease A. *Biochemistry* **1996**, *35*, 1548−1559.
(47) Zscherp, C.; Aygün, H.; Engels, J. W.; Mäntele, W. Effect of Proline to Alanine Mutation on the Thermal Stability of the All-β-Sheet Protein Tendamistat. *Biochim. Biophys. Acta, Proteins Proteomics* **2003**, *1651*, 139−145.
(48) Reimer, U.; Mokdad, N. E.; Schutkowski, M.; Fischer, G. Intramolecular Assistance of Cis/Trans Isomerization of the Histidine−Proline Moiety. *Biochemistry* **1997**, *36*, 13802−13808.